LINC

Learning about Interacting Networks in Climate

Marie Curie Initial Training Networks (ITN)

FP7- PEOPLE - 2011- ITN

Grant Agreement No. 289447

WorkPackage WP4: *Future Climate Change*

Deliverable D4.4

Report on changes in teleconnections from the tropics in a global warming scenario

Marcelo Barreiro, Universidad de la República, Uruguay

Release date: 15 December 2014

Status: *public*

EXECUTIVE SUMMARY

In the Deliverable D4.2 we reported about our advances in understanding the influence of the global tropical oceans on precipitation over Southeastern South America during spring time. The main finding was that this influence shows interdecadal variability and that different oceans play the most important role at different times of the 20th century, even though the equatorial Pacific dominates.

In Deliverable D4.3 we reported about the evolution of the global atmospheric connectivity at upper levels during the 20th century centering the analysis on the 200 hPa eddy geopotential field. This field is particularly important for the transmission of the influence from the tropics toward the extratropics in the form of Rossby wave teleconnection patterns. We found that the most connected regions are on the tropics over the Pacific ocean and that the southern hemisphere extratropics have more connectivity in the first half of the 20th century. Moreover, results suggest that the main connectivity pattern captured in the reanalysis networks are due to the oceanically-forced component, particularly on interannual time scales, and that the atmospheric internal variability seems to play an important role in determining the intraseasonal time scale networks.

The above results pose clear questions regarding as to why are there periods of increased connectivity and synchronization, and why are they characterized by different roles of the ocean basins. We presented a first hypothesis related to the strength of the variability in each basin and are currently understanding the physical processes. Here we present the results of an analysis to determine whether these periods of synchronization may change their characteristics in a future scenario of climate change. We found that under a rcp8.5 scenario there will be a decrease of the synchronization among the network's components. Thus, the tropical oceans and rainfall variability over southeastern south America will become more disconnected in the future consequence of anthropogenic forcing.

Deliverable Identification Sheet

Grant Agreement No.	**PITN-GA-2011-289447**
Acronym	**LINC**
Full title	**Learning about Interacting Networks in Climate**
Project URL	http://climatelinc.eu/
EU Project Officer	Lucia PACILLO

Deliverable	**D4.4 Report on the identification of processes associated with climate shifts in the S.H.**
Work package	**WP4 Future Climate Change**

Date of delivery	**Contractual**	M 36	**Actual**	16-12-2014
Status	version. 1.00		final ☑	draft
Nature	Prototype	Report ☑	Dissemination	
Dissemination Level	Public	Consortium ☑		

Authors (Partner)	**Marcelo Barreiro, Universidad de la Republica, Uruguay**			
Responsible Author	Marcelo Barreiro		**Email**	**barreiro@fisica.edu.uy**
	Partner	Universidad de la Republica	**Phone**	

Abstract (for dissemination)	Report on the Deliverable 4.4 of WP4 of the LINC project.	
Keywords	Climate change, rainfall, southern hemisphere, projections, synchronization	

Table of Contents

1 INTRODUCTION

Several previous studies have shown different atmospheric and oceanic teleconnections through which the tropical Pacific, Atlantic and Indian Oceans can interact among them (e.g., Enfield *et al.*, 1996; Chiang and Sobel, 2002; Meyers *et al.*, 2007; Annamalai *et al.*, 2003; Wang and Wang, 2014). In turn, other studies have found that these tropical oceans influence rainfall variability over Southeastern South America (SESA) through different physical mechanism (e.g., Yulaeva and Wallace, 1994; Grimm *et al.*, 2000; Silvestri, 2004; Mo and Berberly, 2011 and Chan *et al.*, 2008). However, until recently there were no studies that analyzed how the tropical basins can interact together to influence SESA precipitation variability. Using a methodology from complex networks, Martín-Gómez and Barreiro (2014) constructed a climate network in order to analyze how SESA precipitation variability on spring time is collectively influenced by the interannual variability phenomena that characterize the tropical basins during the 20th century. The network was constructed considering El Niño3.4, the Tropical North Atlantic (TNA), the Indian Ocean Dipole (IOD) and the precipitation over SESA (PCP) indices as nodes, and the mean network distance as a measure of synchronization among them. Their results show that the last century is characterized by the presence of two synchronization periods (30s and 70s) in which the nodes that have effects on SESA precipitation variability changed along the time. Particularly, El Niño 3.4 and the TNA were the interactive which influenced SESA precipitation during the 30s, and El Niño3.4 and the IOD during the 70s.

In this study we construct the same climate network with the aim of evaluating how two climate models used for climate projections (CCSM4 and HadGEM2-ES) can reproduce the observed synchronization of this climate network during the 20th century, and analyze the possible changes resulting from anthropogenic forcing during the 21st century under the rcp8.5 scenario.

In section 2 we introduce the data and methodology used. In section 3 we evaluate how the models used for climate projections reproduce the main features of the network constructed employing the 20th century observations, and describe the main features of the projected climate network for the 21st century considering the more realistic climate model projection. Finally, in section 4 we summarize the results.

2 DATA AND METHODOLOGY.

2.1. Data

We consider the monthly means of SST and precipitation data from 4 ensembles of two different CMIP5 models in order to define the three different tropical oceanic indices and precipitation over Southeastern South America index that represent the network's nodes (see table 1). The election of HadGEM2-ES in this study is based on the good performance in reproducing precipitation, temperature and other atmospheric fields in the present climate (Cavalcanti et al., 2012). In addition, the CCSM4 model will be also considered.

For both CMIP5 models we consider the historical runs (or 20th century runs) from 1901 to 2004 in order to first check how the model reproduce the statistics of synchronization events observed during the 20th century shown by Martín-Gómez and Barreiro (2014). We focus on the statistics of synchronization events because models generate their own internal dynamics so that particular events will not coincide with those found in observations. We then consider the scenario RCP8.5 during the 21st century, which covers the period from 2005 to 2100 for the case of the CCSM4 model and from 2005 to 2098 in the case of the HadGEM2-ES model.

CMIP5-Model	runs	variable	Resolution	
			latitude	longitude
CCSM4	Historical and 21st century rcp8.5	SST	1.25º	1.25º
		PCP	0.94º	1.25º
HadGEM2-ES	Historical and 21st century rcp8.5	SST	1.25º	1.25º
		PCP	1.25º	1.88º

Table 1. CMIP5 models considered to construct the climate network.

2.2. Methodology

The methodology consists in several steps:

First, we define the climate indices by latitudinally and longitudinally averaging SST and precipitation in the different regions considered (see table 2 and Figure 1). We also eliminate the trend of the time series and compute the monthly anomalies removing the climatological cycle from 1901 to 2004 for the case of the historical run (or 20th century run), and from 2005-2100 or 2005-2098 for the 21st century runs of the CCSM4 and HadGEM2-ES models, respectively. In the case of the Indian Ocean Dipole, we subtract the average between the two boxes to construct the index. The indices are normalized.

Second, we consider individual trimesters to construct the networks: September – November (SON) for the case of El Niño index and October – December (OND) for the rest of the indices (TNA, IOD and PCP). Before taking 3-months mean and in order to avoid aliasing effects, we first apply a low-pass Lanczos Filter (Duchon, 1979) with cutoff frequency of 1/12 to the monthly mean time series. Therefore, the time series have 104 (one per year) for the cases of 20th century runs and 96-94 for the cases of the CCSM4 and HadGEM2-ES 21st century runs.

Third, following the methodology of Martín-Gómez and Barreiro (2014), we construct the network considering the mean network distance as synchronization measure. Mathematically, the mean network distance is defined as:

$$d(t) = \frac{2}{N(N-1)} \sum_{i<j} \sqrt{2\left(1 - \left|\rho_{ij}^{t}\right|\right)} \quad (1) \tag{1}$$

where t denotes the time in the middle of a sliding window of width Δt=11 years, N represents the number of network's nodes (in this case, 4) and is the Spearman correlation coefficient between nodes i and j. The time step for the sliding window is 1 year.

The mean network distance as a measure of synchronization can be interpreted as the average correlation between all possible network's components. Note that the network is completely synchronized when the distance is zero and disconnected when the distance is $\sqrt{(2)}$ (uncorrelated nodes). In turn, equation (1) uses the absolute value of cross correlation because we are interested in knowing when the interactions between two nodes are significant independently of the sign.

Fourth, to compute the statistical significance of the mean network distance we consider the Montecarlo method employing the following criterion: we first compute the autocorrelation coefficient at lag 1 year of each index (remember that each index has one value per year and represents the seasonal mean), and consider as red noise those with autocorrelation coefficient significant at 95% level in one-tailed t-test (white noise in the opposite case). Then, we generate 1000 surrogate time series of each index under these null hypotheses and compute the network distance time series considering a sliding window of 11-years length, as done for the observed indices. In this way, we construct 1000 surrogate time series of the mean network distance, which allows

determining the 5% level. We consider that there is a statistically significant synchronization event when the mean network distance is below this threshold.

This procedure is carried out separately for the 4 ensemble members of the CCSM4 and HadGEM2-ES models and for both runs (historical and 21st century run).

Index short name	Long name index	Earth's region	
		Latitude range	Longitude range
NINO3.4	El Niño3.4	5ºN-5ºS	170ºW-120ºW
TNA	Tropical North Atlantic	10ºN-30ºN	60ºW-30ºW
IOD	Indian Ocean Dipole	10ºS-10ºN 10ºS-0ºN	50ºE-70ºE 90ºE-110ºE
PCP	Precipitation over Southeastern South America (only land areas are considered)	40ºS-25ºS	60ºW-50ºW

Table 2. Geographical regions that represent the network's nodes. The indices are defined considering the spectral average of the sea surface temperature and precipitation anomalies in the specified regions. In the Indian Ocean Dipole case, the index is computed from the difference between the 2-D average SST in the west and the 2-D average in the east region. Regions are plotted in Figure 1.

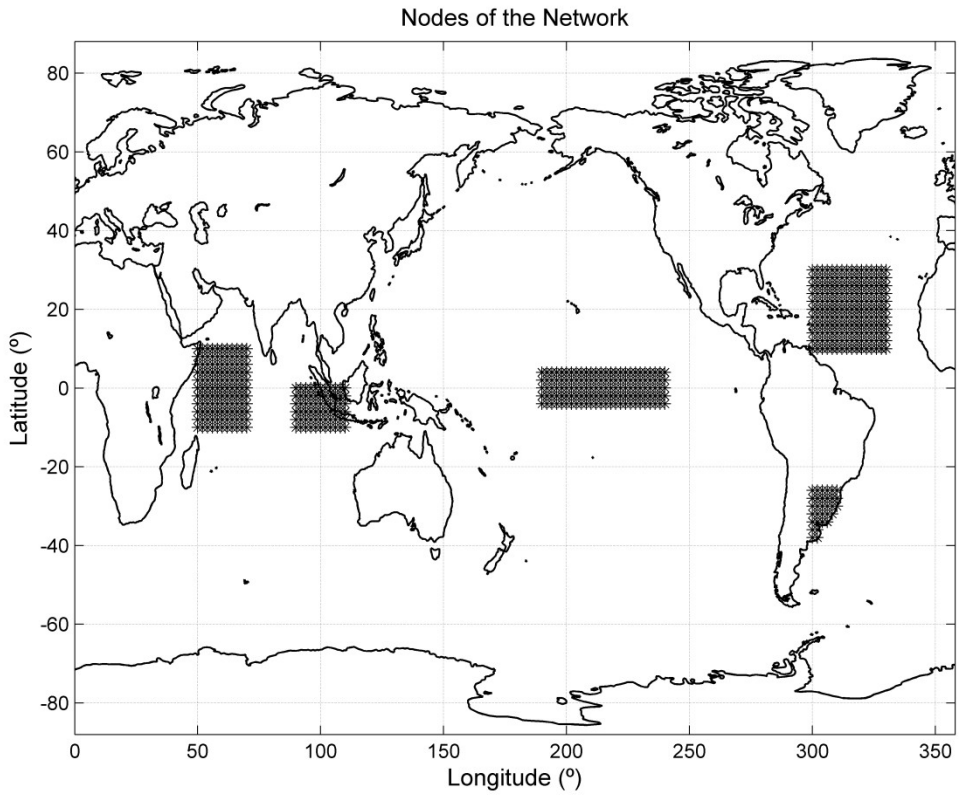

Figure 1. Regions that represents the climate indices: Indian Ocean Dipole (IOD) over the Indian Ocean, Niño3.4 over the central equatorial Pacific Ocean, the Tropical North Atlantic (TNA) and the precipitation over Southeaster South America (PCP).

After that, we evaluate the skill of the models reproducing the statistics of synchronization during the 20th century. The one that reproduces best will provide more confidence in the future climate projections. To evaluate how the model reproduce the statistics of observed synchronization during the last century we focus on six different features of the network distance: frequency (number of synchronization periods), time lapse (sum of the total years considering all the synchronization periods), maximum value of the network distance, minimum value of the network distance, amplitude (difference between maximum and minimum values of the network distance), and the number of links that each node has (nodes' connectivity). To quantify the number of nodes' links we compute the Spearman correlation coefficients between each pair of network's nodes (Niño-TNA, Niño-PCP, Niño-PCP, TNA-PCP, IOD-PCP and TNA-

IOD) for each synchronization period and check the statistical significance considering one tailed t-test at 95% confidence level. The criterion that establishes if two network nodes are interacting is the following: (1) We take a period ("window") that corresponds to the years in which the network distance is under the threshold level and compute all the correlation coefficients between the network's nodes. (2) Afterwards, we move the centered-window one year to the left and one year to the right, and compute again the correlation coefficients among the nodes for each moved-window. We say that two nodes are interacting if the three values of the Spearman correlation remain statistically significant.

All the aforementioned network's parameters are calculated for each ensemble member and the results shown here represent the average of the 4 ensembles of each model (the average of the 4 ensemble members for the CCSM4 historical run, the average of the 4 ensembles members for the case of the HadGEM2-ES historical run, and so on…). Finally, it must be mentioned that we only take as synchronization periods those with a number the consecutive synchronized years larger than or equal to 7. We select 7 years-length as a compromise between being a number of years larger than the period of El Niño phenomenon (to allow the SST anomalies variability in the equatorial Pacific) and lower than 10 because we are interesting on the interdecadal variability changes of the mean network distance.

3 RESULTS

3.1 Evaluation of the CCSM4 and HadGEM2-ES models reproducing 20th century synchronization.

In this section we show a comparison between the 20th century run of both CMIP5 models and the results obtained from observations (Figures 2, 3 and 4). Tables 3 and 4

present a summary of the results. Focusing on these two tables, we can see that the main differences between the observations and the models arise mainly from the number of synchronized years per century and the connectivity of each network's node. Overall, while CCSM4 overestimate the number of synchronization periods and synchronized years, the HadGEM2-Es model underestimate them. Nonetheless, the HadGEM2-ES model seems to be the one that presents statistics closer to observations (see in the fifth column of the tables 3 and 4), and our results to analyze the future climate projections will be focusing on this model's output.

	20th Century Observations	**20th Century CCSM4**	**20th Century HadGEM2-ES**	**Model closer to observations**
Number of synchronization periods	2	2.5	1,5	Both models
Number of synchronized years	26	60.25	14,5	HadGEM2-ES
Minimum value network distance	0,8135	0,6977	0,9213	HadGEM2-ES
Maximum value network distance	1,2344	1,2535	1,3036	CCSM4
Amplitude network distance	0,4209	0,5558	0,3823	HadGEM2-ES

Table 3. Main features of the mean network distance during the 20th century for observations (Figure 2) case and the CCSM4 and HadGEM2-ES climate models (Figures 3 and 4). For the case of the models, the value of the variables is computed considering the average of the 4 ensemble members in order to have an average value for 100 years.

Node	**20th Century Observations**	**20th Century CCSM4**	**20th Century HadGEM2-ES**	**Model closer to observations**
Niño3.4	5	7	1	CCSM4
TNA	2	5.25	0.25	HadGEM2-ES
PCP	4	5.25	1	CCSM4
IOD	3	6	1.25	HadGEM2-ES

Table 4. Number of links that each node presents during the 20th century. The number of links for the case of the models is computed as an average of the 4 ensemble members.

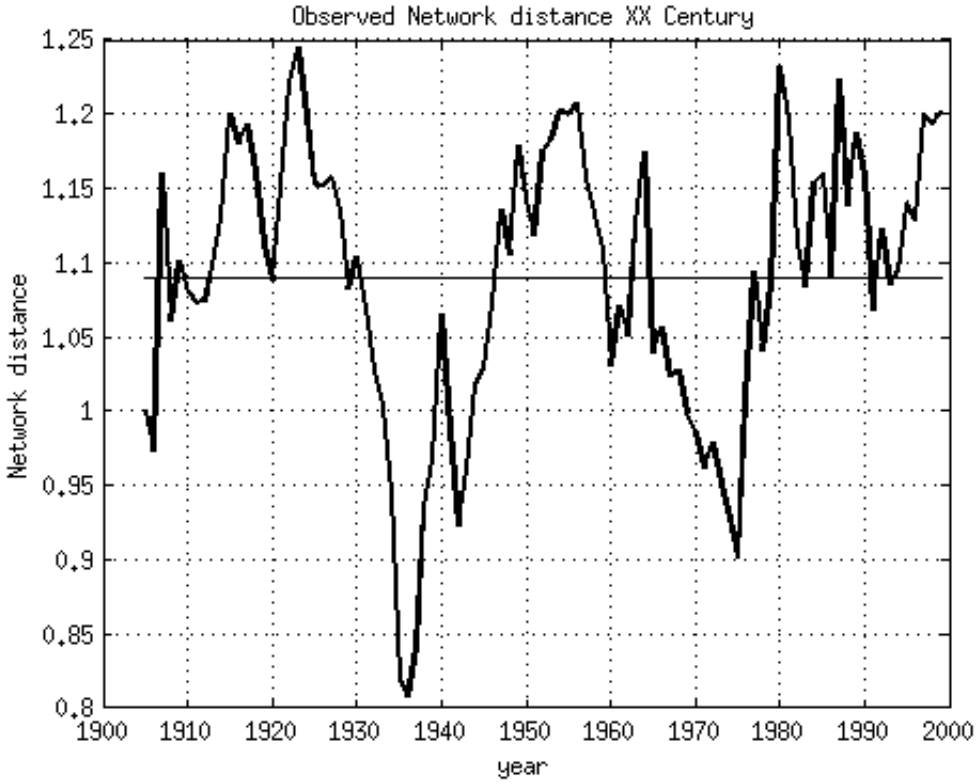

Figure 2. XX Century observed network distance from Martín-Gómez and Barreiro (2014).

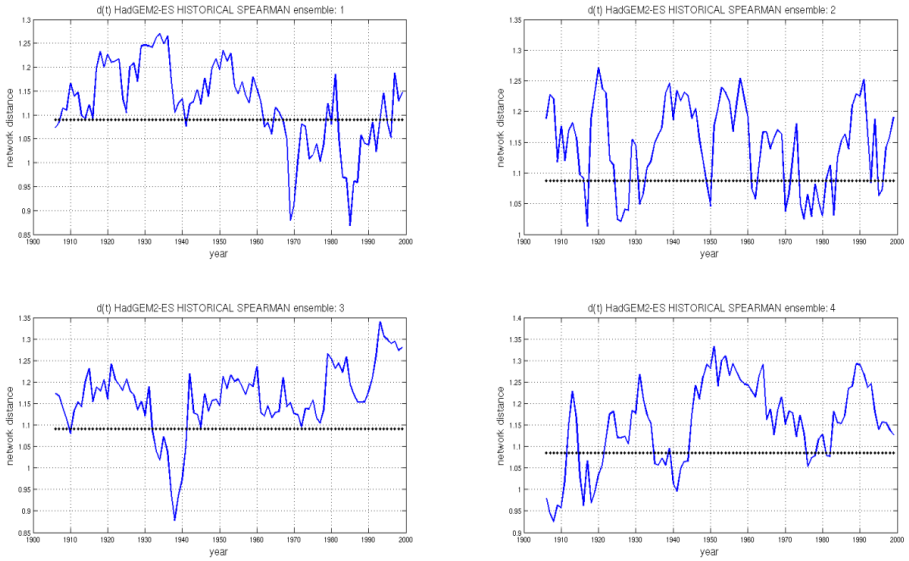

Figure 3. Four ensemble members of historical run (20th century run: 1901-2004) from HaGEM2-ES model.

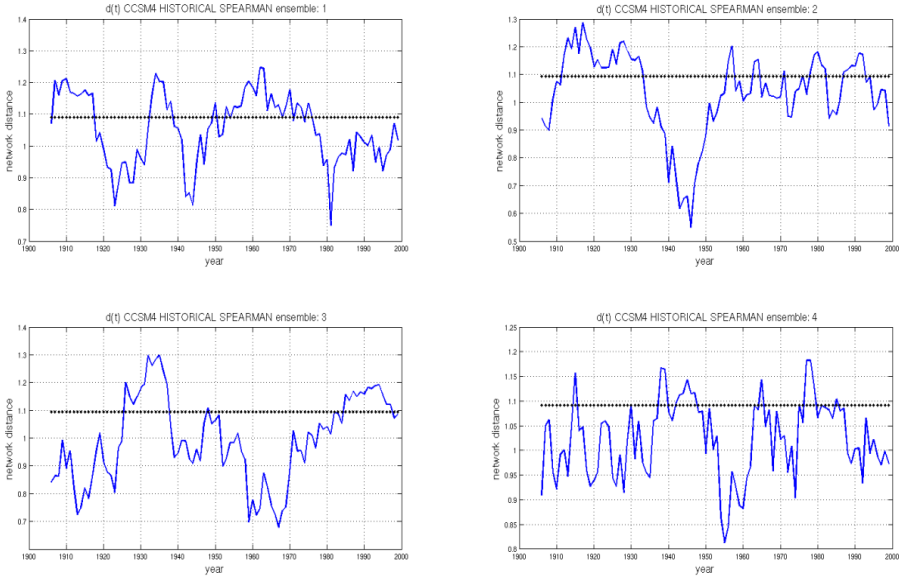

Figure 4. Four ensembles members of the historical run (20th century run: 1901-2004) from CCSM4 model.

3.2 Changes in the network for the 21st century under scenario rcp8.5

In this section we analyze the possible changes that the synchronization among the network's nodes can have during the 21st century under a rcp8.5 scenario of global warming. As it was said before, given that the HadGEM2-ES model tends to be have more skill than CCSM4 in reproducing the observed behavior and it has been shown previously to represent adequately climate variability over south America, our result will be based on this model. The future climate projections of the mean network distances for each ensemble member of HadGEM2-ES are represented in Figure 5.

Tables 5 and 6 present a summary of the main features of the climate network for the 21st century. The main differences among both centuries are in the number of synchronization periods, the years synchronized and the connectivity of each network's component. The number of synchronization periods and the years of synchronization, decrease strongly from 1.5 to 0.5 and from 14.5 to 4.25 respectively. This is directly related to a reduction of the connectivity of the network's nodes (number of links that each node has, Table 6). These results suggest that the anthropogenic forcing will decrease the synchronization among the networks nodes during the next century, being larger the minimum value of the mean network distance for the case of the 21st century. The maximum value, on the other hand, does not seem to vary comparing both centuries.

	20th century HadGEM2-ES	**21th century HadGEM2-ES rcp8.5**
Number of synchronization periods	1,5	0,5
Number of synchronized years	14,5	4,25
Minimum value network distance	0,9213	0,9767
Maximum value	1,3036	1,3156

network distance		
Network distance amplitude	0,3823	0,3389

Table 5. Statistic of the mean network distance and synchronization during the 20th and 21st centuries for HadGEM2-ES model (Figures 2 and 3). Each variable is computed considering the average of the 4 ensemble members in order to have an average value for 100 years. Results from HadGEM2-ES.

Node	20th century HadGEM2-ES	21th century HadGEM2-ES
Niño3.4	1	0,25
TNA	0.25	0
PCP	1	0
IOD	1.25	0,25

Table 6. Number of links that each node presents during the 20th and 21st centuries. The number of links for each case is computed as an average of the 4 ensemble members. Results from HadGEM2-ES.

Although the results of the 21st century run from the CCSM4 are not shown here because its confidence is lower than HadGEM2-ES model, the future projections of the mean network distance calculated with CCSM4 also show a decrease of the synchronization among the network nodes, their connectivity, and the number of synchronized years. This result agreement with those obtained with HadGEM2-ES model, giving more confidence to our previous conclusions.

4 SUMMARY AND CONCLUSIONS

We study how two models used for climate projections can reproduce the synchronization among the tropical oceans and the precipitation over Southeastern South America during the 20th century, in order to project future changes in the network as resulting from anthropogenic forcing during the 21st century under the rcp8.5 scenario.

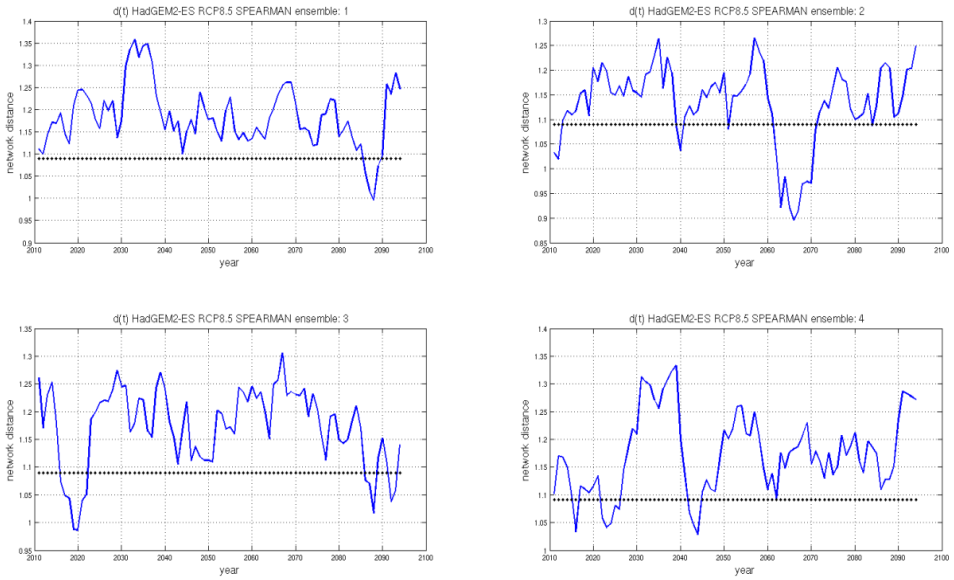

Figure 5. 21st century runs of the mean network distance considering the HadGEM2-ES model's output.

Results show that during the 20th century while the CCSM4 model overestimate the connectivity of the network's nodes and number of synchronization periods and synchronized years, the HadGEM2-ES model underestimates them. Nonetheless, the HadGEM2-ES model shows higher skill in reproducing the observed statistics, and thus it is used to analyze the possible changes in the climate network during the next century. The main results for 21st century under a rcp8.5 scenario suggest a decreasing of the synchronization among the network's components induced by anthropogenic forcing.

5 REFERENCES

Annamalai H, Murtugudde R, Potemra J, Xie SP, Liu P, Wang B. 2003. Coupled dynamics over the Indian Ocean: spring initiation of the zonal mode. *Deep Sea Research II:Tropical Studies in Oceanography*, **50**(12): 2305-2330.

Cavalcanti IFA and Shimizu MH (2012). Climate Fields over South America and Variability of SACZ and PSA in HadGEM2-ES. *American Journal of Climate Change.* vol. 1, p. 132.

Chan SC, Behera SK, Yamagata T. 2008. Indian Ocean Dipole influence on South American rainfall. *Geophysical Research Letters* **35**(14). DOI: 10.1029/2008GL034204.

Chiang JC, Sobel AH. 2002. Tropical tropospheric temperature variations caused by ENSO and their influence on the remote tropical climate. *Journal of Climate* **15:** 2616-2631.

Enfield DB. 1996: Relationships of inter-American rainfall to tropical Atlantic and Pacific SST variability. *Geophysical Research Letters* **23**: 3305–3308. DOI: 10.1029/96GL03231.

Grimm AM, Barros VR, Doyle ME. 2000. Climate variability in Southern South America associated with El Niño and La Niña events. *Journal of Climate* **13**(1): 35-58.

Martín-Gómez V and Barreiro M (2014). Analysis of oceans' influence on spring time rainfall variability over Southeastern South America during the 20th century. Submitted to *International Journal of Climatology.*

Meyers G, Mcintosh P, Pigot L, and Pook M. 2007. The years of El Niño, La Niña and Interactions with the Tropical Indian Ocean. *Journal of Climate* **20**: 2872-2880.

Mo KC, Berbery EH, 2011. Drought and Persistence Wet Spells over South America Base on Observation and the U.S. CLIVAR Drought Experiments. *Journal of Climate.* **24**: 1801-1820. DOI: 10.1175/JCI3874.1

Silvestri GE. 2004. El Niño signal variability in the precipitation over southeastern South America during the austral summer. *Geophysical Research Letters* **31**(18). DOI: 10.1029/2004GL020590.

Wang X, and Wang C. 2014. Different impacts of various El Niño events on the Indian Ocean Dipole. *Climate dynamics* **42**: 991-1005

Yulaeva E, Wallace JM. 1994. The signature of the ENSO in global temperature precipitation fields derived from the Microwave Sounding Unit. *Journal of Climate* **7**:1719-1736.